Express Polymer Letters Vol.17, No.7 (2023) 722–737
Available online at www.expresspolymlett.com
https://doi.org/10.3144/expresspolymlett.2023.54

Research article

Influence of molecular and crosslink network structure on vulcanizate properties of EPDM elastomers

Arshad Rahman Parathodika[1], *Thiyyanthiruthy Kumbalaparambil Sreethu*[1], *Purbasha Maji*[1], *Markus Susoff*[2], *Kinsuk Naskar*[1*]

[1]Rubber Technology Centre, Indian Institute of Technology, 721302 Kharagpur, West Bengal, India
[2]University of Applied Sciences, Osnabrück, Germany

Received 30 November 2022; accepted in revised form 22 February 2023

Abstract. In elastomer science and technology, the advent of vulcanization led to a paradigm change. Despite ongoing research, vulcanization science and technology have a great deal of untapped potential. This article explores how the various vulcanization systems, such as sulfur-based, peroxide-based, and their hybrid systems, would reflect changes in the physio-mechanical characteristics of ethylene-propylene-diene monomer (EPDM) rubber with various molecular configurations. This kind of analysis illuminates the characteristics of the crosslinking network established by each vulcanizing technology. Since solid viscoelastic rubbers include a large number of components, it is nearly impossible to evaluate the crosslinking network directly. If all components other than vulcanizing systems remained intact, stress relaxation behavior correlated directly with the crosslinking network inside the samples. In this work, temperature scanning stress relaxation (TSSR), a relatively new technique capable of creating the whole spectrum of stress relaxation, was effectively explored. The findings suggest that sulfur and carbon crosslinks coexist in hybrid systems regardless of the molecular structure of the elastomer, and their synergistic impact is evident. Furthermore, it is clear from the results that the molecular structure of the vulcanizates has an impact on the final properties, such as tensile, compression strength properties and thermal properties of the samples.

Keywords: *polymer composites, rubber, mechanical properties, temperature scanning stress relaxation, hybrid crosslinking network*

1. Introduction

Vulcanization, often known as curing, is the process by which a two-dimensional entangled polymer chain is crosslinked to form a three-dimensional network. In essence, vulcanization is a physical process that converts plastic polymer chains into an elastic polymer network. Several vulcanization processes have previously been identified and are extensively utilized in business and academics, the most popular of which are sulfur and peroxide-based procedures [1]. Vulcanization restricts the free flow of polymer chains through the formation of network junctions, which also entraps many entanglements. Overall, this results in an elastically active network in the elastomeric chains, which significantly enhances the material's mechanical performance. The type and nature of crosslinking networks developed and their cure sites have a significant role in the final vulcanizate properties of elastomers [2]. The dissociation energy, thermal stability and flexibility of the linkages are prime deciding factors when it comes to the application point of view.

Changes in curing systems are reflected in vulcanizate properties, which are directly related to the network produced in the elastomer if all other components remain the same. Consequently, a systematic examination of the mechanical properties of elastomeric samples in which only the curing systems

*Corresponding author, e-mail: knaskar@rtc.iitkgp.ac.in

vary may provide a significant deal of information about the network produced and their characteristics; the same method is used in this research. Multiple researchers have shown the use of tensile and dynamic mechanical characteristics in elastomer crosslinking network characterization [3]. Although temperature scanning stress relaxation is a relatively recent technique for understanding the relaxation behavior of polymers, the effective use of this technique to comprehend crosslink network characteristics is one of the innovative aspects of our study. In addition, various traditional rubber tests were used to bolster the conclusions of this study.

Polymers subjected to constant strain display the well-known stress relaxation phenomena. Essentially, stress relaxation is a more or less pronounced reduction in stress as a function of time. Physical and/or chemical processes may be responsible for the microscopic factors that contribute to the macroscopic reduction in stress [4]. In thermoset rubbers, chemical processes occurring in the breakage of polymer chains and network junctions govern the thermal-mechanical behavior [5, 6]. Conventionally Maxwell model is used to represent the stress relaxation of viscoelastic solids, but the true behavior of materials is, unfortunately, more complex and cannot be captured by the basic Maxwell model [7]. According to the well-known theory of linear viscoelasticity, the complete relaxation process may be represented using the generalized Maxwell model, which is comprised of an unlimited number of spring-dashpot parts which provide an isothermal relaxation modulus as a function of time. In accordance with Alfrey's rule, the relaxation time constants are inversely proportional to temperature, *i.e.*, the higher the temperature, the lower the relaxation time constants, and vice versa [8–10]. Because the relaxation spectrum spans such a broad time scale, it is almost difficult to identify the complete function from a single measurement of stress relaxation. To generate a master curve based on the time-temperature superposition concept, typically, a series of observations at many temperatures must be performed. Therefore, a great deal of work is necessary to acquire comprehensive information about stress relaxation behavior. Recently, temperature scanning stress relaxation (TSSR) measurements have been used as an alternate method. In contrast to conventional isothermal experiments, the temperature is not held constant during TSSR measurements; rather, it climbs linearly with a constant heating rate. Thus, the non-isothermal relaxation modulus ($E_{\text{non-iso}}$) is derived as a function of temperature. In a manner similar to observations of isothermal stress relaxation, the spectrum $H(T)$ may be approximated using Equation (1) [11–13]:

$$H(T) = -\Delta T \cdot \left(\frac{\mathrm{d}E_{\text{non}-\text{iso}}}{\mathrm{d}T}\right)_{\beta = \frac{\Delta T}{t} = \text{const}} \quad (1)$$

where the relaxation spectrum $H(T)$ is a function that is related to the system's population of relaxation mechanisms, and β is the heating rate of the temperature scan. Despite the fact that this function is not specified on a time scale, the relaxation processes shown by the polymer sample throughout the test may be easily recognized since the relaxation time constant decreases monotonically with rising temperature T. Due to its very high dependency on temperature, the relaxation time constant quickly decreases to negligible values within a short temperature range. Consequently, during the temperature scan of a TSSR test, the whole spectrum can be seen on a temperature scale within a very little time, which was successfully utilized in this study. In TSSR, in addition to stress relaxation, two further processes, namely heat expansion and rubber elasticity of the sample, are considered [14].

In addition to monomers, molecular level features of elastomers, such as molecular weight, monomer ratio, crystallinity, degree of unsaturation, type of branching, entanglement density, and viscosity, may significantly affect the final elastomer product attributes. How these features are represented in the final properties when various vulcanizing processes are used is very seldom addressed comprehensively. This research evaluated the vulcanizate qualities of two ethylene-propylene-diene monomer (EPDM) rubber types from opposite ends of the property spectrum by curing them with four distinct curing processes. EPDM was chosen as the basis matrix for this investigation because sulfur and peroxide-based curing processes have proven effective in commercial applications; another objective of this research is to analyze the behavior of hybrid curing systems. Consequently, the viability and uses of EPDM with both curing systems make it the ideal material for analyzing the features of a hybrid curing system based on sulfur and peroxide.

As previously mentioned, the most sought-after vulcanizing systems are sulfur and peroxide, but in this study, we are also incorporating the relatively new

idea of a hybrid system. In this instance, a hybrid system combines sulfur and peroxide system components, hoping to have a synergistic impact on the qualities of the vulcanizate. Carbon-sulfur-carbon linkages are created by sulfur vulcanization and are renowned for their excellent flexibility and higher tensile properties. In contrast, carbon-carbon crosslinks are created by peroxide and are renowned for their excellent thermal stability and low compression set properties [15, 16]. Both systems have flaws. Hence a hybrid system is anticipated to eliminate the flaws while combining the positive aspects of both systems. In general, sulfur systems are believed to form crosslinks at allylic positions of double bonds in unsaturated elastomers. In the case of EPDM, only the dimer molecule, Ethylidene norbornene (ENB), has double bonds. Peroxides may generate crosslinks in both the main chain and pendent dimer molecules, as seen in Figure 1. Thus, in a hybrid system, it is envisaged that such linkages would coexist, resulting in a number of alterations to the vulcanizate's characteristics. In addition, during the crosslinking with peroxide, peroxide creates macro radicals (radicals located in the EPDM main chain as a result of hydrogen abstraction). Sulfur is capable of attaching to these radicals and transferring the radical to them, resulting in sulfur crosslinks connecting the main chains of EPDM, which is anticipated to result in significant changes to vulcanizate properties [17]. Many authors discuss the impact of sulfur in the peroxide vulcanization system, with the same conclusion: adding a trace amount of sulfur enhanced the tensile capabilities with a compromise in compression set properties [18–20]. They concluded that the existence of labile sulfur crosslinks explained their findings. Similar research also notes that adding sulfur results in less crosslink density (XLD) due to an interaction between the sulfur and peroxide radicals. Yet it has also been documented that in hybrid curing systems, the high values of crosslink densities show up when stearic acid and zinc oxide are present. Brodsky [19] have found that hybrid systems had higher tensile strength than sulfur vulcanizates and tear strength that is on par with sulfur vulcanizates. The effect of two-stage curing was reported previously [21]. Engelbert [22] showed that the mechanical qualities of EPDM might be enhanced by curing it using a combination of sulfur-peroxide and sulfur-electron beams. In addition, Chakraborty *et al.* [23] comprehensively evaluated several investigations covering a wide range of mixed curing systems. Cumuloxy radical annihilation in a sulfur/peroxide hybrid crosslinking system was reported by Banerjee and coworkers [20, 24–26] Kruželák and coworkers [27, 28] investigated the effect of curing system composition on crosslinking and physical and mechanical properties of acrylonitrile butadiene rubber (NBR) samples. They found that samples

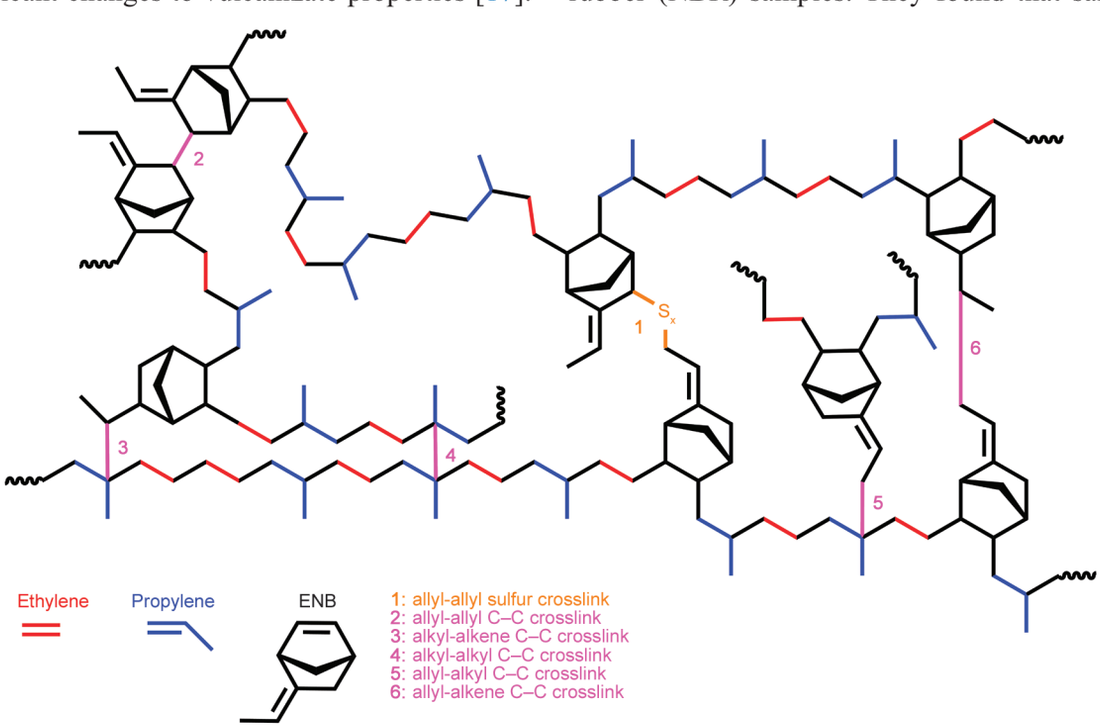

Figure 1. Schematic displaying various sulfur and carbon-carbon linkages observed in EPDM rubbers.

cured with an equivalent ratio of sulfur and peroxide had the highest tensile strength and elongation at break and that thermooxidative aging improved the physical-mechanical properties of vulcanizates based on NBR regardless of curing system composition. Nakason *et al*. [29] used the sulfur-peroxide hybrid cure technique to crosslink epoxidized natural rubber (ENR)/ polypropylene (PP) thermoplastic vulcanizates (TPVs). They reported that hybrid-cured TPVs showed greater mixing torques, shear stress, shear viscosity, tensile strength, and elongation at break than sulfur and peroxide-cured systems. Moreover, hybrid-cured TPVs had higher dispersed ENR particle sizes.

In essence, this research investigates the interrelationship between the molecular network structure of EPDM and the previously described vulcanizing systems (sulfur, peroxide, and hybrid systems) by comparing the physio-mechanical characteristics of vulcanizates. In detail, two grades of EPDM elastomers with entirely different molecular structures and attributes were selected to determine each cure system's disparate reactions to the distinct molecular structures of EPDM. In addition to two optimized hybrid systems, a commercially established sulfur system and a peroxide system were employed as vulcanizing systems in this investigation. Testing specimens of samples were produced based on both the EPDM grades using these four curing methods. A thorough analysis of the physio-mechanical responses of the samples derived the inter-relationship of the vulcanizate network and molecular structure in EPDM rubber.

2. Experimental

2.1. Materials

Two varieties of EPDM elastomers named Keltan 10675C DE and Keltan 4465 are procured from ARLANXEO Performance Elastomers, Changzhou City, China. Of which Keltan 10675C DE is a highly crystalline grade with 65 wt% ethylene content, 6.0 wt% ENB and a high Mooney viscosity of 67 MU(ML(1+8) 150 °C). In addition, this grade has controlled long-chain branching, which contributes to high performance and better processing properties. It also contains 50 phr of high-quality, colorless extender oil, making it an excellent grade for low-hardness rubber products that require excellent UV resistance. However, the Keltan 4465 is mostly amorphous with an ethylene content of 56 wt%, ENB content of 4.1 wt%, and a Mooney of 48 Mooney unit (MU) (ML(1+4) 125 °C). This grade is of broad molecular weight distribution and 50 phr oil extension, which make it suitable for low hardness profiles. As per observed Mooney values, Keltan 10675C DE is predicted to have 1.5 times the molecular weight of Keltan 4465 and 10675C DE and 4465 grades have specific gravities of 0.86 and 0.87 kg/dm^3, respectively, as determined by the ASTM D 297–15 method. Perkadox 14-40B-PD-S (peroxide), a 40% active organic peroxide (Di[tert-butylperoxyisopropyl] benzene) from Nouryon, Amsterdam, The Netherlands, functions as a major vulcanization agent in this study. Zinc oxide (ZnO) and sulfur are obtained from Merck India Limited, Mumbai, India. All other rubber compounding ingredients say stearic acid, polymerized 2,2,4-trimethyl-1,2dihydroquinoline (TQ), and the vulcanization accelerators such as 2-mercaptobenzothiazole (MBT) and tetramethyl thiuram disulfide (TMTD) are procured from NOCIL India Limited, Mumbai, India. Merck India Limited (Mumbai, India), provided the cyclohexane solvent used in the swelling investigation. PCBL Limited's (Gujarat, India) N-550 grade fine extrusion furnace carbon black is also used in this investigation. Each component is used in its original form; those susceptible to absorbing moisture are dried in an oven before use.

2.2. Methodology

The experimental part of this study started with the preparation of masterbatches based on Keltan 10675C DE and Keltan 4465 according to the formulations shown in Table 1 at 145 °C and 60 rpm. Henceforth, they will be known as the HM series and LM series, respectively. After 24 hours of maturation, vulcanizing chemicals are integrated into the masterbatch using the same Haake™ Rheomix OS, a lab-sized internal mixer, at room temperature. The finished compound is sheeted in a two-roll mill, and its vulcanization time and other rheological characteristics are assessed using an MDR 2000 type moving die rheometer. Throughout the mixing process, ASTM D3182-21a is adhered to, and standard vulcanized sheets and test specimens are produced in a compression molding press from the final compound in line with the standards provided in the respective sections.

Table 1. Composition of samples present in this study in phr.

Ingredients	SHM-1	HHM-1	HHM-2	PHM-1	SLM-1	HLM-1	HLM-2	PLM-1
Keltan 10675 C DE*	150	150	150	150	–	–	–	–
Keltan 4465*	–	–	–	–	150	150	150	150
ZnO	3	3	3	–	3	3	3	–
Stearic acid	1	1	1	–	1	1	1	–
TQ	1	1	1	1	1	1	1	1
Carbon black (N 550)	70	70	70	70	70	70	70	70
MBT	0.5	0.5	0.5	–	0.5	0.5	0.5	–
TMTD	1	1	1	–	1	1	1	–
Sulfur	1.5	0.5	0.5	–	1.5	0.5	0.5	–
Perkadox 14-40 BPD	–	1.5	3	6	–	1.5	3	6

*50 phr oil extended elastomer

2.3. Characterization of samples

2.3.1. Mooney viscosity

The Mooney viscosity of raw rubbers was determined in accordance with ASTM D 1646 using a Mooneyline viscometer manufactured by Prescott Instruments (Tewkesbury, UK) with a big rotor at 125 °C. The results are analyzed to determine the type of basic elastomers.

2.3.2. Rheometeric studies

Disc-shaped specimens with a volume of approximately 5 cm^3 are cut from the final compound using a volumetric sample cutter. They are subjected to an isothermal cure study at 170 °C in Monsanto MDR 2000 (Akron, USA), with an oscillation arc of ±0.5° for 30 minutes. In addition to vulcanization features such as optimum cure time (TC_{90}), cure rate index (*CRI*), and delta torque, the rate constants of vulcanization are derived from this data.

2.3.3. Temperature scanning stress relaxation

The temperature-dependent stress relaxation behavior of samples was examined using a TSSR Meter (Brabender, Duisburg, Germany). The specimens are dumbbell-shaped (Type 5A, ISO 527) and were punched from a 2 mm thick compression-molded sheet. The specimens are kept in an electrically heated test chamber at 23 °C and a 50% strain is applied in the first stage. In the second phase, the sample is held at 50% strain for two hours to diminish short-term relaxation mechanisms. In the third phase, the non-isothermal test was conducted by gradually increasing the temperature at a rate of 2 °C/min until the stress relaxation was complete or the sample rupture. A schematic view of the test procedure is given in Figure 2.

A thermocouple near the specimen center detected its temperature in real-time. High-quality signal amplifiers and analog-to-digital (AD) converters were utilized to detect and digitize force transducer and thermocouple analog signals. All signals were transmitted to a computer, where software treated and evaluated the data and controlled the test operation. The results include force ratio, which is the quotient $F(T)/F(0)$. $F(T)$ and $F(0)$ indicate the force at temperature T and T_0, respectively. T_{10}, T_{50}, and T_{90} are determined from the normalized force-temperature curve, as shown in Figure 2. Here, the T_{90} could be used to measure the degree of thermo-oxidative chain breakdown of polymers. TSSR index (*RI*) is derived from the area under the normalized force-temperature curve, indicating the elastic behavior of the material (Equation (2)). The crosslink density of the samples can be obtained from TSSR(CLD-TSSR) based on the theory of rubber elasticity [30]:

$$RI = \frac{\int_{T_0}^{T_{90}} \frac{F(T)}{F_0} \mathrm{d}T}{T_{90} - T_0} \tag{2}$$

2.3.4. Mechanical properties

2 mm thick sheets are prepared from the final compound using compression molding. ASTM D 412-C type of dumbbell specimens are punched from the sheet, and tensile strength is measured at 25±2 °C in a Hioks-Hounsfield UTM (Test Equipment Ltd, Surrey, England) at a crosshead speed of 500 mm/min. The presented findings are the average of three specimens per sample. Furthermore, the hardness of all samples is measured from 6 mm thick disc specimens using a Shore A durometer.

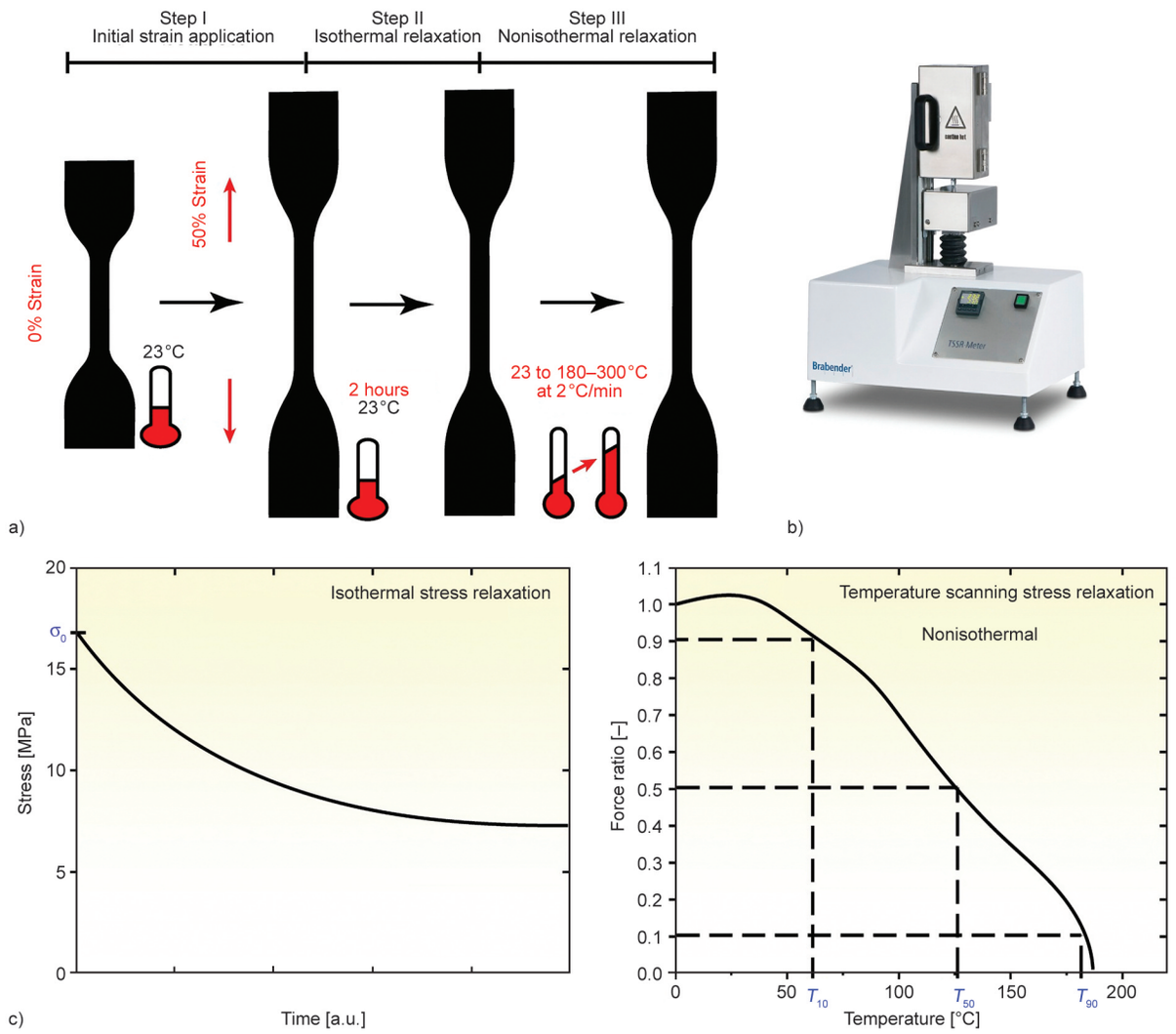

Figure 2. a) Schematic view of the test procedure, b) TSSR instrument, c) and conventional plots from TSSR.

2.3.5. Compression set

Method B under ASTM D 395 is used throughout the test. A cylindrical specimen with a thickness of 6 mm and a diameter of 13 mm is molded directly and used for the measurements. The cylindrical specimens were compression-molded using a vulcanization time of TC_{90} + 5 minutes to ensure that heat was evenly distributed throughout the thickness. The specimens are compressed in spacers that can maintain a constant deflection of 25% of the initial thickness for 70 hours at 100 °C. The initial and final thicknesses are measured using a thickness gauge, and the percentage compression set is computed using Equation (3). The stated results for the compression set are the mean of three specimens per sample:

$$\textit{Compression set}\,[\%] = \frac{T_{\text{Initial}} - T_{\text{Final}}}{T_{\text{Initial}} - T_{\text{Spacer}}} \cdot 100 \qquad (3)$$

where T is the thickness, T_{Initial}, T_{Final}, are the thickness of the sample before and after compression set experiments, also T_{Spacer} is the thickness of the spacer used for the experiment.

2.3.6. Heat aging

Vulcanized sheets of 2 mm thickness were heat-aged at 100 °C for 72 hours in a hot air oven.

Change in tensile properties

The tensile properties of the samples are tested before and after heat aging in accordance with ASTM D 412. The percentage change in properties is calculated from Equation (4):

$$\Delta P[\%] = \frac{P_{\text{after ageing}} - P_{\text{before ageing}}}{P_{\text{before ageing}}} \cdot 100 \qquad (4)$$

where P refers to the tensile properties such as tensile strength, elongation at break, modulus.

Dynamic mechanical analysis (DMA)

In tensile mode, strain sweep measurements are conducted using 20×5 mm strips punched from a 2 mm thick vulcanized sheet. This test is used to analyze the aging behavior of the samples, strips from aged and unaged samples are tested, and the results are compared. The strain sweep is performed in the dynamic strain range of 0.01 to 20% at a frequency of 10 Hz in Metravib 50N France at 50 °C. Parameters such as storage modulus (E'), loss modulus (E''), and tan delta (tan δ) are obtained from this study.

2.3.7. Swelling studies

Using swelling tests in cyclohexane for 72 h at 25±2 °C, crosslink density was determined. The analysis uses 2 mm thick disk-shaped vulcanized specimens. Equation (5) was used to calculate the volume fraction of swollen rubber (V_r). Where m_1 and m_2 are the dry polymer and solvent swollen sample weights, while ρ_1 and ρ_2 are their densities. Test specimens were weighed before swelling, after swelling, and after drying and then using the Flory–Rehner equation (Equation (6)), crosslink density (ν) was calculated. V_s refers to cyclohexane's molar volume, which is 107.7 cm^3/mol. Flory-Huggins polymer-solvent interaction parameter (χ) of EPDM-Cyclohexane used was 0.38 [31]. It can be noted that when comparing compounds with the same filler content, relative crosslink density values can be compared without Kraus adjustment [32, 33]:

$$V_r = \frac{Volume\ of\ rubber}{Volume\ of\ rubber + Volume\ of\ solvent} = \frac{\frac{m_1}{\rho_1}}{\frac{m_1}{\rho_1} + \frac{m_2}{\rho_2}} \quad (5)$$

$$\nu = -\frac{1}{2V_s} \cdot \frac{\ln(1 - V_r) + V_r + \chi V_r^2}{V_r^{1/3} - \frac{V_r}{2}} \quad (6)$$

3. Results and discussion

3.1. Mooney viscosity

The sole difference between the two series of samples in this analysis is their base elastomers. Mooney viscosity is therefore utilized as a tool to investigate their fundamental differences in molecular structure [34]. Figure 3 depicts the Mooney viscosity plot of both base elastomers, revealing that the HM series base elastomer has a Mooney value of 76.8 MU, which is twice as large as the LM series base elastomer Mooney viscosity under similar test conditions. The Mooney value clearly shows that the HM series base elastomers have a larger molecular weight and a lower polydispersity index than the LM series base elastomer. Furthermore, it suggests the existence of more long-chain ethylene crystallites in HM series base elastomer. In all the performance properties of the vulcanizates in this study, the effect of this fundamental difference in molecular structure can be observed.

3.2. Rheometric studies

The curing behavior of samples was analyzed at 170 °C on a Monsanto moving die rheometer. Table 2 summarizes the critical cure parameters derived from the rheo curves (Figure 4), such as scorch time (TS_2), maximum torque (M_H), delta torque (ΔS: measured as the difference between maximum and minimum torque), cure time (TC_{90}: time taken to attain 90% maximum torque) and cure rate index [35].

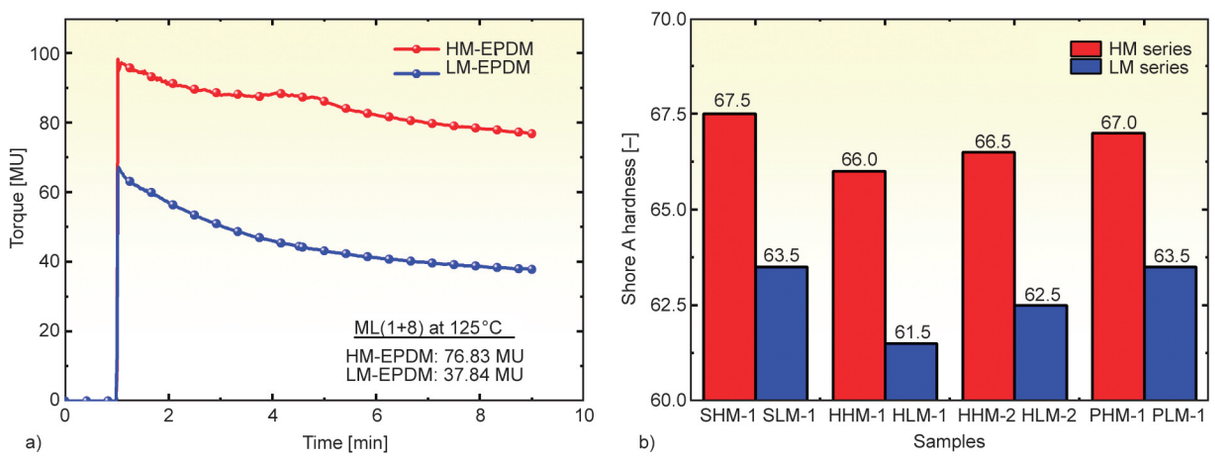

Figure 3. a) Mooney viscosity of two grades of EPDM used, b) Shore A hardness of the samples.

Table 2. Vulcanization parameters obtained from Monsanto moving die rheometer MDR 2000.

Sample	TS_2 [min]	M_H [dN·m]	Delta torque [dN·m]	TC_{90} [min]	*CRI* [–]
SHM-1	0.89	20.32	17.70	10.27	10.66
HHM-1	1.23	16.01	13.02	8.97	12.91
HHM-2	1.12	16.17	13.19	8.44	13.68
PHM-1	0.76	19.71	16.57	11.09	9.69
SLM-1	1.21	15.58	13.65	11.19	10.02
HLM-1	1.47	12.03	10.09	8.90	13.46
HLM-2	1.39	12.66	10.69	9.31	12.63
PLM-1	1.11	15.26	13.18	13.09	8.35

Figure 4 illustrates the difference between the HM and LM series' rheological behavior. The maximum torque value difference between the HM and LM series remains relatively consistent regardless of the curing technique (4.17±0.47 dN·m). This indicates that none of these curing systems induce significant scission or breakage in the main chain of the elastomers; instead, crosslinking is the predominant response that occurs here. It can also be noted that the elastomeric chain network structure and their branching type are different for both series. Aside from this, when comparing the HM and LM series, the other curing metrics, such as TC_{90} and *CRI*, exhibit no noticeable change.

Within a series, the essential cure parameters of both hybrid systems in the HM and LM series are comparable, indicating that only a small proportion of peroxide is directly involved in the crosslinking process. However, the samples are also brought to the subsequent investigations in order to comprehend the function of this additional peroxide in determining the cure site and the impact of sulfur on peroxy radical destruction. Based on the comparable M_H and delta torque values of sulfur-based and peroxide-based samples in both series (SHM-1 *vs*. PHM-1 and SLM-1 *vs*. PLM-1), it can be inferred that both curing methods are capable of producing network structure at 170 °C. However, the hybrid systems exhibit lower M_H and delta values of around 3.5 units in both series. This difference is often linked to decreased network density and the degree of recovery. It is expected because the likelihood of peroxy radical destruction is high, and it restricts the availability of components for the vulcanization process. However, in the case of hybrid systems, this is not the case because, as seen in Table 1, unlike sulfur- or peroxide-based systems,

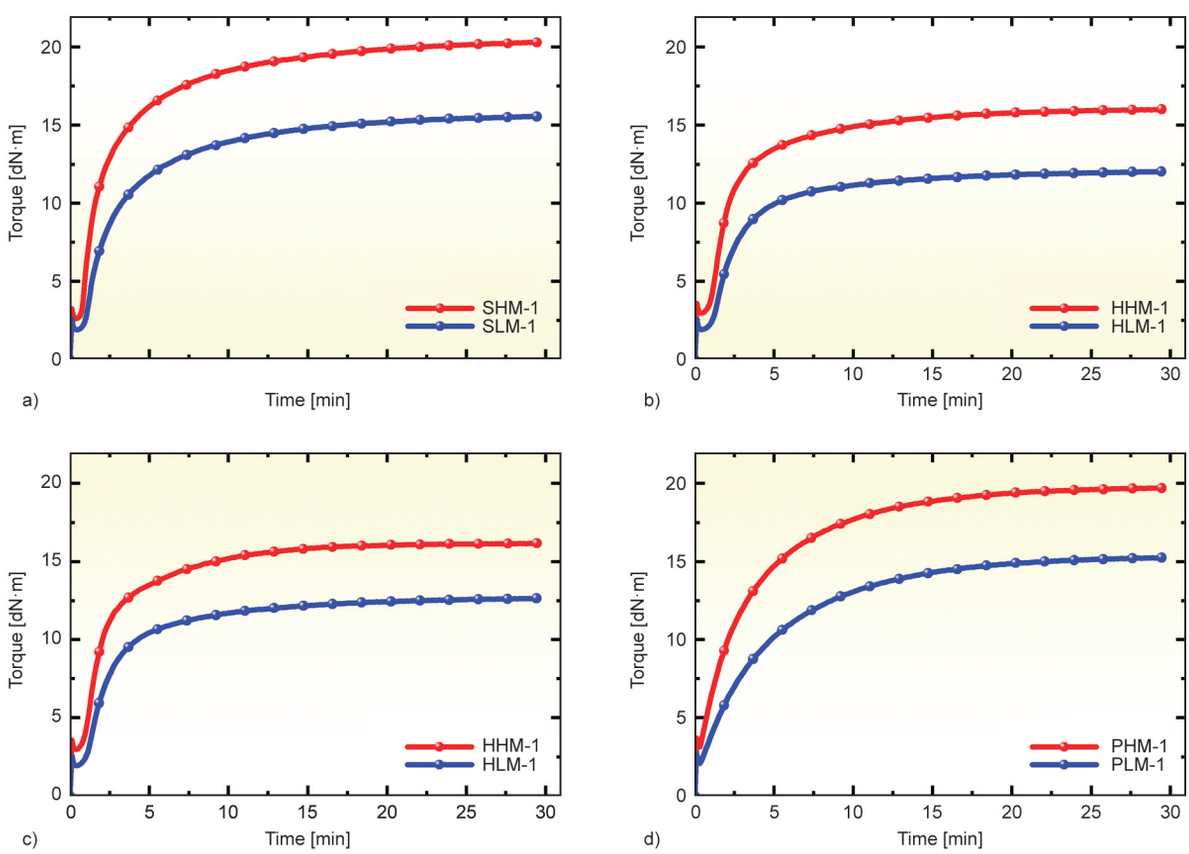

Figure 4. Vulcanization rheo plots of a) sulfur, b) and c) hybrid and d) peroxide-based systems at 170 °C.

hybrid systems use less vulcanization chemicals; these recipes are proved to perform best in our previous investigation [17]. In addition, it contradicts the notion that hybrid systems have better performance characteristics, as will be shown in the following sections.

3.3. Temperature scanning stress relaxation

Figures 5c and 5d, depict the stress-temperature curves from TSSR for the HM series and LM series, respectively. The normalized force temperature curves are shown in a similar fashion in Figures 5a and 5b. Normalized force versus temperature curves of HM series samples features a strong initial rise in force, which may be ascribed to the improved entropy effect of HM series base elastomer (EPDM-Keltan 10675 C DE) owing to regulated long chain branching. In turn, this improves their mechanical performance to levels equivalent to natural rubber. In addition, samples from the LM series also exhibit the first rise in the force-temperature curve, although it is gradual and similar to curves described by other authors [36]. In TSSR plots, one of the most significant differences between the HM and LM series is that some of the LM series sample force values decay by more than 50% at higher temperatures, but the HM series decay is smaller. This is because the LM series base elastomer (EPDM-Keltan 4465) has a low molecular weight and a higher polydispersity index. Detail-wise, the low molecular weight and high polydispersity index of the LM series base elastomer indicate the presence of polymeric chains of varying lengths, of which shorter chains are typically not assumed to form elastically active entanglements; furthermore, they tend to slip over other chains and enhance the stress relaxation process. However, the presence of rigid carbon-carbon crosslinks, in essence, creates the effect of higher molecular weight, and the difference is evident in the case of the PLM-1 sample. In detail, Table 3 summarizes the key parameters from TSSR. In line with the classical theory of rubber elasticity for unfilled compounds, the Neo-Hookean rule (Equation (7)) holds, and the stress (σ)

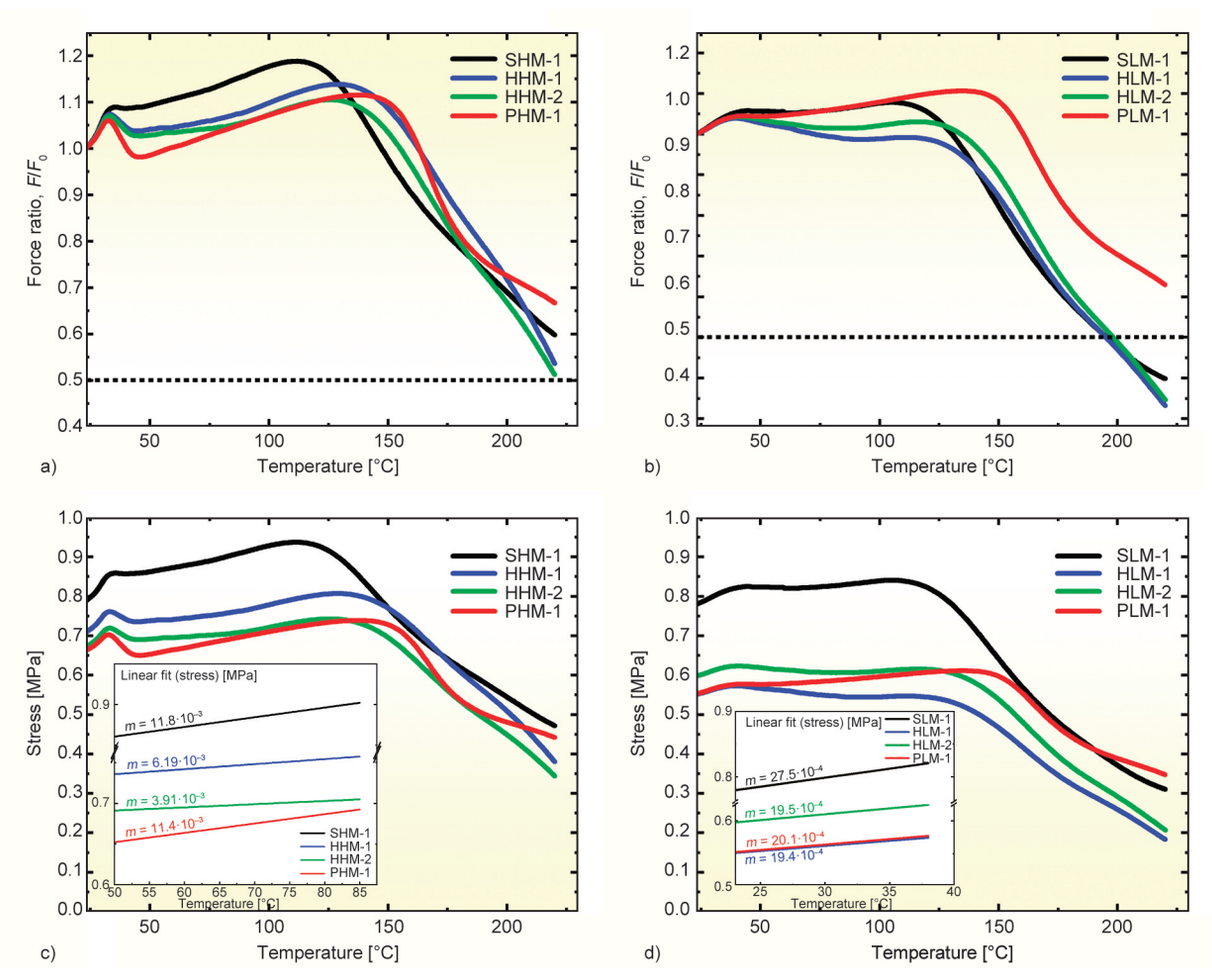

Figure 5. Normalised force ratio curve of a) HM series b) LM series stress *vs* temperature curve of c) HM series d) LM series, on insight the slope of stress vs temperature curve.

is proportional to the crosslink density of the network (ν):

$$\sigma = \nu \cdot R \cdot T \cdot (\lambda - \lambda^{-2}) \quad (7)$$

where R is the universal gas constant, T is the temperature, and λ (strain ratio) = l/l0, where l is the sample length and l0 is the sample's initial length. The stress temperature coefficient K for a constant λ is provided by Equation (8):

$$K = \left(\frac{d\sigma}{dT}\right)_{\lambda} = \nu \cdot R \cdot (\lambda - \lambda^{-2}) \quad (8)$$

From this crosslink density can be obtained using Equation (9):

$$\nu = \frac{K}{R \cdot (\lambda - \lambda^{-2})} \quad (9)$$

To extend this model to filled rubber compounds, λ is substituted with Λ and the reinforcing component ϕ is added (Equation (10)):

$$\Lambda = \epsilon \cdot \phi + 1 \quad (10)$$

where ϵ represents the relative strain and the factor of reinforcement (ϕ) is defined by $\phi = 1 + 2.5V_f + 14.1V_f^2$ (V_f: volume fraction of filler). It is evident from Equation (8) that the slope of the stress *versus* temperature curve is correlated to the crosslink density of samples [37]. Such plots can be produced using TSSR (see Figures 5c and 5d), and the slope at low temperatures is taken into account when estimating crosslink density since sulfur-based and carbon-carbon crosslinks are stable at these temperatures. In this work, the crosslink density of samples is determined using the stress-temperature plot from TSSR. In this way of examination, the crosslink density values of LM series samples are somewhat lower. It is due to the greater number of elastically active entanglements in the HM series due to its longer chain length.

When comparing samples within a series, it is fascinating to see their deconvoluted relaxation spectra (Figure 6). Monosulfidic and polysulfide connections are represented by two different peaks in sulfur-cured materials. In contrast, peroxide samples have a single signal, which corresponds to carbon-carbon bonds. In addition, the hybrid system exhibits three peaks, which indicates the co-existence of sulfidic and carbon-carbon bonds. The peak temperature correlates to the temperature stability of individual crosslink bonds. Therefore it can be shown that polysulfide linkages have a temperature resistance of 147 °C (Figure 6a Peak 1) and monosulfide linkages have a temperature resistance of 200 °C (Figure 6a Peak 2). In contrast, peroxide-induced carbon-carbon bonds have a temperature resistance

Table 3. Critical parameters from TSSR analysis.

Sample	σ_0 [MPa]	T_{10} [°C]	T_{50} [°C]	TSSR index	Crosslink density* [mol/m^3]
SHM-1	0.79	160.6	–	0.99	1180.0
HHM-1	0.71	175.1	–	0.99	619.0
HHM-2	0.67	167.4	–	0.96	391.8
PHM-1	0.66	171.1	–	0.98	1140.6
SLM-1	0.78	142.4	195.5	0.87	275.6
HLM-1	0.55	143.2	195.2	0.84	194.0
HLM-2	0.60	150.5	198.3	0.87	195.1
PLM-1	0.55	169.6	–	0.98	201.4

*These values are obtained from TSSR

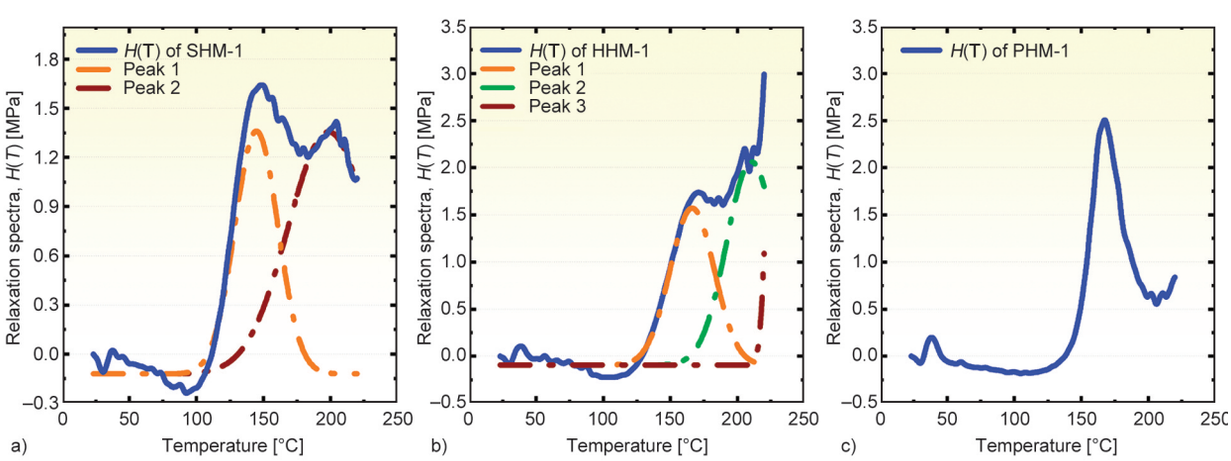

Figure 6. Relaxation spectra from TSSR of a) sulfur cured (SHM-1) b) hybrid cured (HHM-1) and c) peroxide cured (PHM-1) samples.

of 170 °C. The deconvoluted relaxation spectrum of a hybrid treatment has three peaks at 164, 205, and 212 °C. The peak at 164 °C corresponds to polysulfide links, while the peaks at 205 and 212 °C relate to monosulfide and carbon-carbon connections; however, it is difficult to discriminate between them. The increased temperature resistance of polysulfide and monosulfide links may be attributable to the likelihood of sulfur linkage formation in the backbone of EPDM elastomer in hybrid systems as opposed to pure systems. Relaxation spectra of the LM series also follow the same trend. In addition, based on the T_{10} values, hybrid cure systems have better temperature stability. The T_{10} values for hybrid cure systems rise by 14.5 and 4 °C compared to sulfur and peroxide systems, respectively, indicating greater network formation and slower relaxation in hybrid systems.

The TSSR index may be used to examine the elasticity of samples; the greater the TSSR index, the greater the elasticity of the rubber network [6, 38]. Greater elasticity within a certain elastomer grade correlates to greater network density and/or strength, as well as a higher number of entrapped entanglements. The phrase 'entrapped entanglement' refers to entanglements that got imprisoned as a result of the creation of crosslinks. Detailing polymers composed of high molecular weight chains made of repeating units. Due to microscopic Brownian motions, polymer chains get entangled with one another. Models of random walking explain this occurrence. However, when strain is given to an uncrosslinked polymer, the chains flaw and tend to align, resulting in a decrease in entanglement. However, when a polymer undergoes crosslinking, the free movement of chains is constrained, many entanglements are protected or imprisoned, and they help the polymer to improve its elasticity, and they are called elastically active entrapped entanglements. The TSSR index values of samples indicate that all HM series samples have similar TSSR index values. With the exception of peroxide-cured samples, the same pattern reappears in the LM series as well. In comparing the TSSR index of both series, all samples in the HM series have a value close to one, indicating their high elasticity, whereas the LM series has a value of 0.86, indicating that the LM series has inferior elastic properties compared to the HM series, with the exception of the peroxide-cured LM sample.

3.4. Swelling studies

The crosslink densities of the samples were also determined using swelling, followed by the Flory Rehner equation (Equation(6)). Figure 7 crosslink density values derived from swelling experiments and TSSR. The fluctuation of vulcanizate characteristics with crosslink density has been the subject of several investigations [39]. In general, characteristics such as tensile, tear, and fatigue life improve with increasing crosslink density until they reach a maximum, at which point they tend to decrease with additional increases in crosslink density. In contrast, some characteristics, such as dynamic modulus and compression set, continue to improve as crosslink density increases. Several papers provide potential reasons for this phenomenon [40, 41]. There are many forms of intermolecular and intramolecular crosslinks as well as network defects, such as dangling chain ends and chain loops. However, only chemical crosslinks that are elastically active and entanglements that are trapped will contribute to the physical qualities.

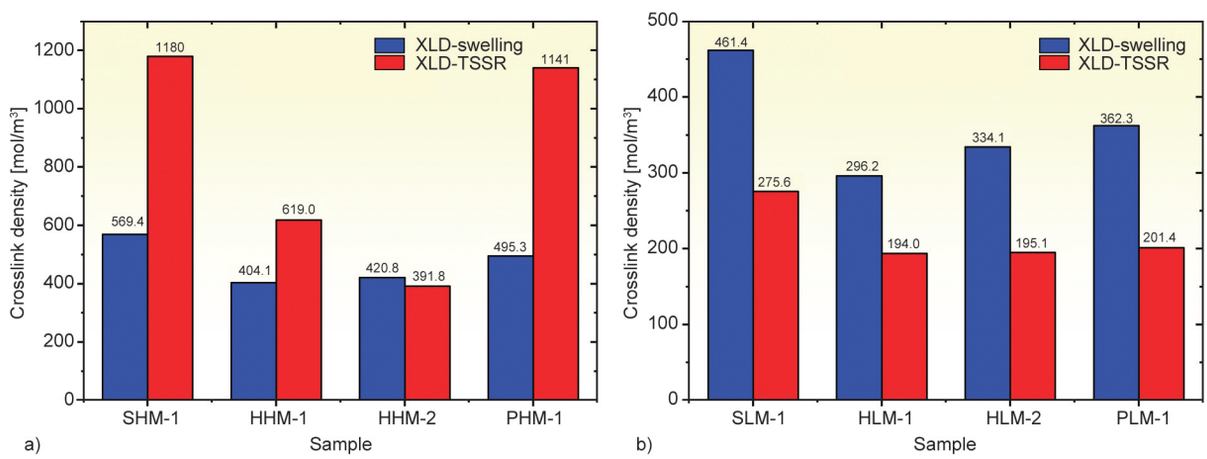

Figure 7. Crosslink densities from swelling study and TSSR meter for a) HM series b) LM series.

Consequently, it is not required that an increase in crosslink density would optimize all vulcanizate qualities in the same manner as delta torque. In both TSSR and swelling studies, the findings of this study indicate that the crosslink density of samples from the HM series is greater than that of samples from the LM series. It is due to the increased molecular weight and entanglement density of the HM series elastomer, in essence, both the measurement methods quantify the crosslink density based on the physical response. The second significant difference between the series is that, whereas in the HM series, TSSR measurement exhibits higher values than swelling, in the LM series, swelling experiments exhibit higher values than the TSSR. Comparing samples within a series reveals that both the HM and LM series exhibit a similar pattern of delta torque values, indicating that the majority of torque development during vulcanization is due to the generation of crosslinks in the rubber matrix. Both sulfur- and peroxide-based systems exhibit greater crosslink density values than hybrid systems in both series. However, the superior performance of hybrid systems could be attributed to their versatile options for cure sites. Comparing sulfur, hybrid, and peroxide systems, the crosslink density value trends from TSSR and swelling are in agreement. However, the crosslink density values of the two hybrid systems exhibit a little deviation from the trend between TSSR and swelling. Moreover, swelling experiments reveal a smaller variation in crosslink density between pure and hybrid systems, whereas TSSR demonstrates an approximately two-fold difference. In general, all of the crosslink density values presented are comparable to the crosslink density values of existing EPDM compounds of commercial interest, which are documented in a number of studies.

3.5. Mechanical properties

The vulcanizate qualities, such as tensile and dynamic capabilities, can provide a fair indication of the crosslinked network and its structure. Aside from that, it is generally accepted that a lower crosslink density, which is above a critical crosslink density, will be more effective at blunting the crack tips than a higher crosslink density. It is because a higher crosslink density restricts segmental motion, thereby reducing the ability of the chains to respond to the crack [42]. Figures 8 represents the tensile properties of the samples. Moreover, the HM series base elastomer (EPDM-Keltan 10675 C DE) is a growing alternative to natural rubber. Using hybrid vulcanization systems, the HHM-1 sample has a tensile strength of 25.9 MPa, which outperforms the standard-filled natural rubber compounds. Tensile strength data shows that all samples in the HM series are stronger than the LM series irrespective of the curing system used, which can be attributed to the high molecular weight of the base elastomer, their controlled long chain branching and their high crystalline nature due to the presence of ordered polyethylene chain segments. However, the LM series samples show higher elongation at break values than the HM series, which correlates to their high amorphous nature and low viscosity. Similar filler content is utilized throughout the samples; consequently, a similar reinforcement index is anticipated. Nearly all of the samples exhibit a similar reinforcement index, except for pure peroxide samples, which can be attributed to the higher concentration of rigid carbon-carbon crosslinking bonds in peroxide samples. Interestingly, both sulfur-cured and hybrid-cured samples have comparable values of 100 and 200% modulus values. On the other hand, both times, the peroxide samples have a higher modulus value for the HM series. However,

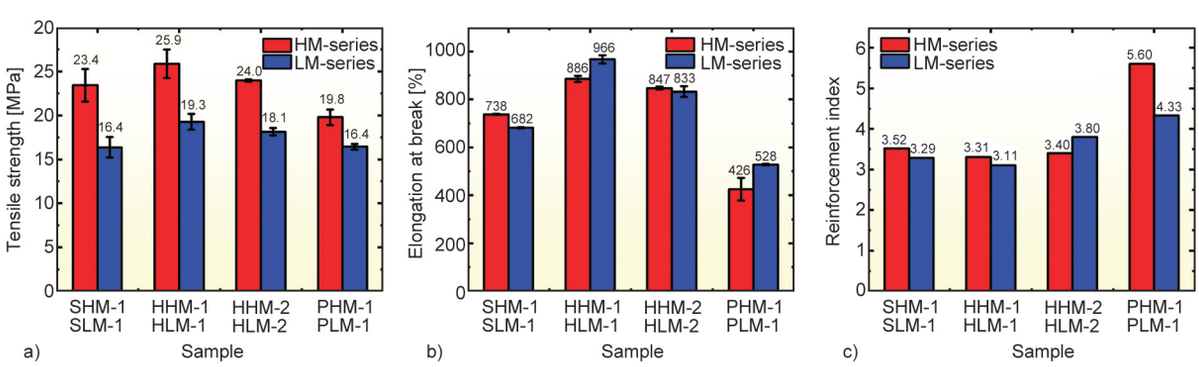

Figure 8. Bar plots of a) tensile strength, b) elongation at break, c) reinforcement index.

the 300% modulus values of both series differ greatly, and in most cases, the HM series shows a higher value. Regardless of the series, when comparing the tensile strength and elongation at break of samples within a series, both hybrid samples outperform pure sulfur and peroxide systems. This is a significant accomplishment of the study, which is anticipated to occur owing to the hybrid system's extra sulfur cure sites. As the hybrid system exhibits much greater tensile and elongation capabilities than the pure system, the modulus values of the hybrid system are somewhat smaller than those of the pure system, which is predicted owing to the hybrid system's high chain segmental motion. In contrast, peroxide samples have a greater reinforcement index and lower elongation at break than hybrid and pure sulfur systems. In essence, hybrid compounds have enhanced tensile qualities relative to their counterparts.

3.6. Compression set

Compression set at a lower temperature is exactly proportional to crosslinking density, regardless of the kind of crosslink, since at lower temperatures, almost crosslinks have the same impact, taking their thermal stability into account [43]. Comparing compression set values across series reveals that samples from the HM series had a lower compression set value for all curing processes, which is advantageous. As in the prior situation, it may be linked to their molecular structure. Moreover, the trend of compression set values of samples in both series is the same, indicating that this feature is directly connected to the crosslinked network generated rather than elastomers' intrinsic properties. Compression set values of all samples are represented in Figure 9a. While comparing the compression set values of samples, it can be shown that the hybrid system shows a mediocre value between the sulfur and peroxide systems, which further indicates the presence of the co-existence of both sulfur and carbon-carbon linkages. To make a rough estimate based on the compression set values, it can be proven that a hybrid system creates around 65% sulfur crosslinks, and the rest are carbon-carbon linkages. As both series continue to show this pattern, the theory becomes more compelling.

3.7. Heat aging

The thermal stability of the network formed during vulcanization is evaluated during a heat aging test, which can then be used to predict how the material would function and deteriorate in a real application. Samples age when subjected to high temperatures over extended periods of time, and as a result, less thermally stable polysulfide crosslinks rearrange to mono or di-sulfidic connections. Even if there is an improvement in properties, a more significant shift from initial values has no positive effects, which causes alterations in the characteristics of the system

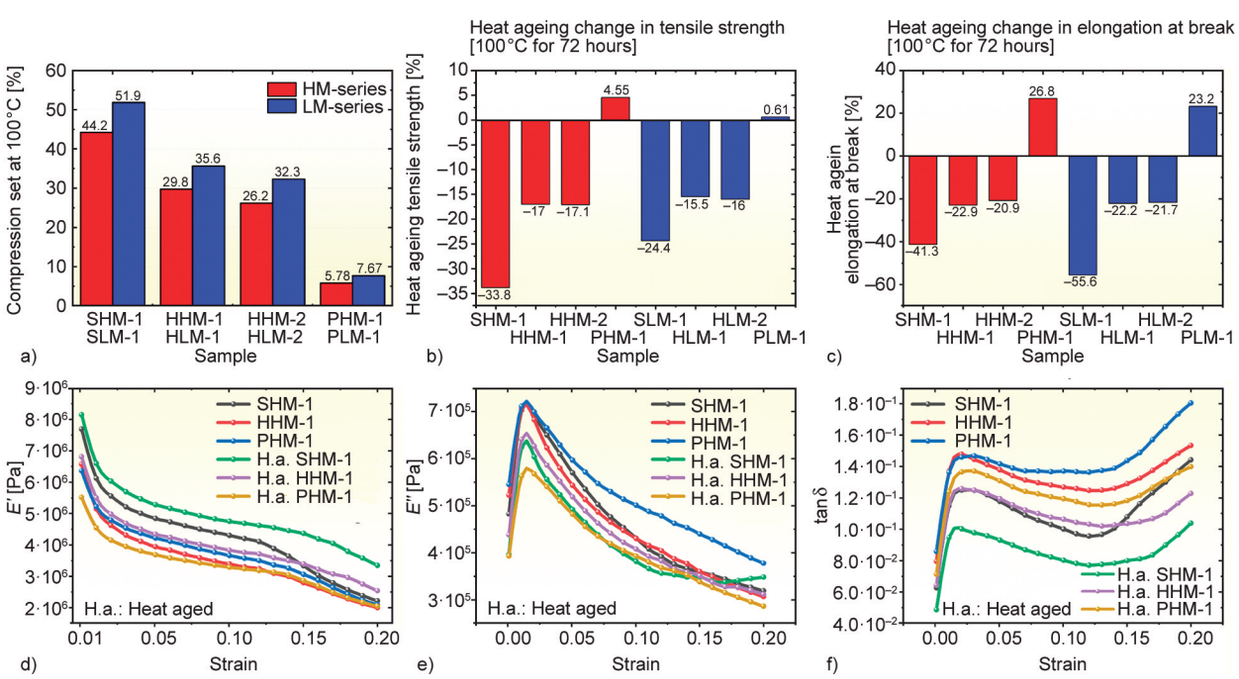

Figure 9. Bar plots of a) compression set, b) change in tensile strength, c) heat aging change in elongation at break, and d) strain sweep storage modulus plot e) strain sweep loss modulus plot f) tan δ from DMA.

in which the article functions. In this research, samples are examined for their tensile qualities and their strain sweep behavior under the dynamic circumstances specified in the characterization section. Then, they were aged at 100 °C for 72 hours, and their tensile characteristics and strain sweep behavior were examined again to determine the impact of aging on the crosslinked network. Figures 9b and 9c represents the variation of properties in tensile characteristics after heat aging, both series follow the same pattern, and the sulfur vulcanizates tensile properties degrade more, and the peroxide sample tensile properties increase little, as anticipated and described in the literature. In addition, when compared to sulfur vulcanizates, hybrid systems exhibit superior performance and 50% less degradation. This again confirms the presence of both carbon linkages and sulfur linkages in hybrid systems. Figure 9d–9f depicts the results of DMA strain sweep measurements. Three samples from the HM series are investigated in this study, and the findings indicate that sample SHM-1 exhibits a reduction in the Payne effect, which is connected with the rearrangement of polysulfide links to monosulfide linkages. However, the hybrid system (HHM-1) shows similarity to the peroxide system (PHM-1), which exhibits an increase in the Payne effect upon aging. As all samples have a comparable filler component, the variance in the Payne effect is mostly attributable to network structure and type.

4. Conclusions

The physio-mechanical characteristics of two grades of EPDM elastomers vulcanized using a sulfur cure system, a peroxide cure system, and two hybrid systems were evaluated. Responses from samples were correlated with the crosslink network in the samples, and the influence of the molecular structure of EPDM in various curing systems was apparent. Temperature-scanning stress relaxation is utilized as the primary instrument to comprehend the network structure of both elastomer grades. In the TSSR relaxation spectrum, it has been shown that sulfur, peroxide, and hybrid cures produce distinct kinds of networks. In essence, a hybrid cure shows the co-existence of both the carbon linkages and sulfur linkages. Similarly, the crosslink density values of samples from swelling studies validate the TSSR findings. In addition, it was intriguing to discover that, regardless of the base elastomer grade, the trend of crosslink density values and the network type were identical, although the TSSR measurement and swelling studies in both grades exhibited distinct absolute values. The physical behavior of the samples in tensile mode and compression mode also validates the results of TSSR. The hybrid samples, in which multiple kinds of crosslinks coexist, overcome the deficiencies of each system and exhibit better behavior in terms of overall qualities. A heat aging test was conducted to confirm the thermal stability of the formed crosslinking bonds and determine the application potential of the hybrid system. All samples performed as expected in the heat aging test based on their constituent crosslink bonds, with the hybrid positioned between the best-performing peroxide-based samples and the worst-performing sulfur-based samples. Overall, the study demonstrates the utility and application potential of a hybrid system with the help of findings about various types of crosslink networks, the co-existence of dual networks, and their stable behavior regardless of the molecular structure of EPDM. In addition, it illuminates the newly developed high-molecular-weight EPDM grade and its exceptional performance characteristics.

Acknowledgements

The authors are grateful to IIT Kharagpur for supporting this work. The authors also thank the Science and Engineering Research Board (SERB) India for funding this work gratefully (Grant Number: CRG/2020/000059 dated 29-12-2020).

References

[1] Akiba M., Hashim A. S.: Vulcanization and crosslinking in elastomers. Progress in Polymer Science, **22**, 475–521 (1997). https://doi.org/10.1016/S0079-6700(96)00015-9

[2] Loo C. T.: High temperature vulcanization of elastomers: 2. Network structures in conventional sulphenamide-sulphur natural rubber vulcanizates. Polymer, **15**, 357–365 (1974). https://doi.org/10.1016/0032-3861(74)90177-3

[3] Aprem A. S., Joseph K., Thomas S.: Recent developments in crosslinking of elastomers. Rubber Chemistry and Technology, **78**, 458–488 (2005). https://doi.org/10.5254/1.3547892

[4] Meng F., Pritchard R. H., Terentjev E. M.: Stress relaxation, dynamics, and plasticity of transient polymer networks. Macromolecules, **49**, 2843–2852 (2016). https://doi.org/10.1021/acs.macromol.5b02667

[5] Vennemann N.: Characterization of thermoplastic elastomers by means of temperature scanning stress relaxation measurements. in 'Thermoplastic elastomers' (eds.: El-Sonbati A. Z.), IntechOpen, Rijeka, Vol. 1, 347–370 (2012). https://doi.org/10.5772/35976

[6] Chatterjee T., Vennemann N., Naskar K.: Temperature scanning stress relaxation measurements: A unique perspective for evaluation of the thermomechanical behavior of shape memory polymer blends. Journal of Applied Polymer Science, **135**, 45680 (2018). https://doi.org/10.1002/app.45680

[7] Johnson A. R., Quigley C. J.: A viscohyperelastic maxwell model for rubber viscoelasticity. Rubber Chemistry and Technology, **65**, 137–153 (1992). https://doi.org/10.5254/1.3538596

[8] Treloar L. R. G.: The physics of rubber elasticity. Clarendon Press, Oxford (1975).

[9] Flory P. J.: Statistical mechanics of swelling of network structures. The Journal of Chemical Physics, **18**, 108–111 (1950). https://doi.org/10.1063/1.1747424

[10] Eichinger B. E.: Rubber elasticity: Solution of the James-Guth model. Physical Review E, **91**, 052601 (2015). https://doi.org/10.1103/PhysRevE.91.052601

[11] Anagha M. G., Chatterjee T., Naskar K.: Assessing thermomechanical properties of a reactive maleic anhydride grafted styrene-ethylene-butylene-styrene/thermoplastic polyurethane blend with temperature scanning stress relaxation method. Journal of Applied Polymer Science, **137**, 49598 (2020). https://doi.org/10.1002/app.49598

[12] Banerjee S. S., Natarajan T. S., Subramani B. E., Wießner S., Janke A., Heinrich G., Das A.: Temperature scanning stress relaxation behavior of water responsive and mechanically adaptive elastomer nanocomposites. Journal of Applied Polymer Science, **137**, 48344 (2020). https://doi.org/10.1002/app.48344

[13] Barbe A., Bökamp K., Kummerlöwe C., Sollmann H., Vennemann N., Vinzelberg S.: Investigation of modified SEBS-based thermoplastic elastomers by temperature scanning stress relaxation measurements. Polymer Engineering and Science, **45**, 1498–1507 (2005). https://doi.org/10.1002/pen.20427

[14] Vennemann N., Schwarze C., Kummerlöwe C.: Determination of crosslink density and network structure of NR vulcanizates by means of TSSR. Advanced Materials Research, **844**, 482–485 (2014). https://doi.org/10.4028/www.scientific.net/AMR.844.482

[15] Loan L. D.: Mechanism of peroxide vulcanization of elastomers. Rubber Chemistry and Technology, **40**, 149–176 (1967). https://doi.org/10.5254/1.3539040

[16] Naskar K., Noordermeer J. W. M.: Dynamically vulcanized PP/EPDM blends: Effects of different types of peroxides on the properties. Rubber Chemistry and Technology, **76**, 1001–1018 (2003). https://doi.org/10.5254/1.3547766

[17] Parathodika A. R., Raju A. T., Das M., Bhattacharya A. B., Neethirajan J., Naskar K.: Exploring hybrid vulcanization system in high-molecular weight EPDM rubber composites: A statistical approach. Journal of Applied Polymer Science, **139**, e52721 (2022). https://doi.org/10.1002/app.52721

[18] Das C. K., Banerjee S.: Studies on dicumyl peroxide vulcanization of styrene – butadiene rubber in presence of sulfur and 2-mercaptobenzothiazole. Rubber Chemistry and Technology, **47**, 266–281 (1974). https://doi.org/10.5254/1.3540436

[19] Brodsky G. I.: Mixed peroxide-sulfur curing system for rubbers. in 'ACS Rubber Meeting, Orlando, USA' 1–28 (1993).

[20] Manik S. P., Banerjee S.: Sulfenamide accelerated sulfur vulcanization of natural rubber in presence and absence of dicumyl peroxide. Rubber Chemistry and Technology, **43**, 1311–1326 (1970). https://doi.org/10.5254/1.3547331

[21] Roland C. M., Warzel M. L.: Orientation effects in rubber double networks. Rubber chemistry and technology, **63**, 285–297 (1990). https://doi.org/10.5254/1.3538259

[22] Bevervoorde-Meilof E.W.E., Haeringen-Trifonova D., Vancso G., Does L., Bantjes A., Noordermeer J.: Crosslink clusters: Reality or fiction?. KGK-Kautschuk und Gummi Kunststoffe,**53**, 426–433 (2000).

[23] Chakraborty S. K., Bhowmick A. K., De S. K.: Mixed cross-link systems in elastomers. Journal of Macromolecular Science Part C, **21**, 313–332 (1981). https://doi.org/10.1080/00222358108080020

[24] Manik S. P., Banerjee S.: Determination of chemical cross-links in rubbers. Die Angewandte Makromolekulare Chemie: Applied Macromolecular Chemistry and Physics, **6**, 171–178 (1969). https://doi.org/10.1002/apmc.1969.050060117

[25] Manik S. P., Banerjee S.: Studies on dicumylperoxide vulcanization of natural rubber in presence of sulfur and accelerators. Rubber Chemistry and Technology, **42**, 744–758 (1969). https://doi.org/10.5254/1.3539254

[26] Manik S. P., Banerjee S.: Studies on sulfur vulcanization of natural rubber accelerated with diphenylguanidine both in presence and absence of dicumyl peroxide. Journal of Applied Polymer Science, **15**, 1341–1355 (1971). https://doi.org/10.1002/app.1971.070150605

[27] Kruželák J., Sýkora R., Hudec I.: Sulfur and peroxide curing of rubber compounds based on NR and NBR. Part I: cross-linking and physical-mechanical properties. Kautschuk Gummi Kunststoffe, **70**, 27–33 (2017).

[28] Kruželák J., Sýkora R., Hudec I.: Sulfur and peroxide curing of rubber compounds based on NR and NBR. Part II: Thermooxidative ageing. Kautschuk Gummi Kunststoffe, **70**, 41–47 (2017).

[29] Nakason C., Wannavilai P., Kaesaman A.: Effect of vulcanization system on properties of thermoplastic vulcanizates based on epoxidized natural rubber/polypropylene blends. Polymer Testing, **25**, 34–41 (2006). https://doi.org/10.1016/j.polymertesting.2005.09.007

[30] Vennemann N., Bökamp K., Bröker D.: Crosslink density of peroxide cured TPV. Macromolecular Symposia, **245–246**, 641–650 (2006). https://doi.org/10.1002/masy.200651391

[31] Zhao Q., Li X., Gao J.: Aging of ethylene–propylene–diene monomer (EPDM) in artificial weathering environment. Polymer Degradation and Stability, **92**, 1841–1846 (2007). https://doi.org/10.1016/j.polymdegradstab.2007.07.001

[32] Dijkhuis K. A. J., Noordermeer J. W. M., Dierkes W. K.: The relationship between crosslink system, network structure and material properties of carbon black reinforced EPDM. European Polymer Journal, **45**, 3302–3312 (2009). https://doi.org/10.1016/j.eurpolymj.2009.06.029

[33] Kraus G.: Swelling of filler-reinforced vulcanizates. Journal of Applied Polymer Science, **7**, 861–871 (1963). https://doi.org/10.1002/app.1963.070070306

[34] Nakajima N., Harrell E. R.: Method of obtaining viscosity curves with mooney rheometer. Rubber Chemistry and Technology, **52**, 9–19 (1979). https://doi.org/10.5254/1.3535212

[35] Babu R. R., Singha N. K., Naskar K.: Dynamically vulcanized blends of polypropylene and ethylene-octene copolymer: Comparison of different peroxides on mechanical, thermal, and morphological characteristics. Journal of Applied Polymer Science, **113**, 1836–1852 (2009). https://doi.org/10.1002/app.30076

[36] Bhattacharya A. B., Gopalan A. M., Chatterjee T., Vennemann N., Naskar K.: Exploring the thermomechanical properties of peroxide/*co*-agent assisted thermoplastic vulcanizates through temperature scanning stress relaxation measurements. Polymer Engineering and Science, **61**, 2466–2476 (2021). https://doi.org/10.1002/pen.25772

[37] Blume A., Kiesewetter J.: Determination of the crosslink density of tire tread compounds by different analytical methods. Kautschuk Gummi Kunststoffe, **72**, 33–42 (2019).

[38] Uthaipan N., Junhasavasdikul B., Vennemann N., Nakason C., Thitithammawong A.: Investigation of surface properties and elastomeric behaviors of EPDM/EOC/PP thermoplastic vulcanizates with different octene contents. Journal of Applied Polymer Science, **134**, 44857 (2017). https://doi.org/10.1002/app.44857

[39] Blow C. M.: Rubber technology and manufacture. Butterworths for the Institution of the Rubber Industry, London (1971).

[40] Beek W., Willink D., Aa P., Nijhof L.: Hybrid cure systems for EPDM and EPM - based on organic peroxide-accelerated sulfur. Gummi Fasern Kunststoffe, **70**, 98–108 (2017).

[41] Maiti M., Patel J., Naskar K., Bhowmick A. K.: Influence of various crosslinking systems on the mechanical properties of gas phase EPDM/PP thermoplastic vulcanizates. Journal of Applied Polymer Science, **102**, 5463–5471 (2006). https://doi.org/10.1002/app.25106

[42] Hamed G. R.: Effect of crosslink density on the critical flaw size of a simple elastomer. Rubber chemistry and technology, **56**, 244–251 (1983). https://doi.org/10.5254/1.3538117

[43] Martin G., Barrès C., Cassagnau P., Sonntag P., Garois N.: Viscoelasticity of randomly crosslinked EPDM networks. Polymer, **49**, 1892–1901 (2008). https://doi.org/10.1016/j.polymer.2008.02.003